Journal of Marine Science and Technology (2021) 26:233–242
https://doi.org/10.1007/s00773-020-00735-4

ORIGINAL ARTICLE

A simpler approach to analysis ship maneuvering performances of hybrid propulsion ship using a HILS

Sung-An Kim[1]

Received: 28 February 2020 / Accepted: 2 May 2020 / Published online: 16 May 2020
© The Japan Society of Naval Architects and Ocean Engineers (JASNAOE) 2020

Abstract
A simulation verification of the hybrid propulsion ship considering accurate electro-dynamic model is required to evaluate ship maneuverability before the maritime demonstration. This paper presents the simplified model constructions for the hybrid propulsion ship using a real time simulator in terms of the dynamic models accuracy and the improvement of a computation speed. In addition, the hardware in the loop simulator based on a laboratory virtual instrument engineering workbench using the ship dynamic model and the developed equipment is proposed to evaluate the electro dynamic characteristics of hybrid propulsion ship. The validity of a proposed model on a hardware in the loop simulator is verified by simulation compared with a detailed model on an electronic circuit simulation software.

Keywords Hardware in the loop simulator · Hybrid propulsion ship · Hybrid electric power system · Hybrid power supply system · Ship maneuverability

1 Introduction

In accordance with the Kyoto protocol of the united national convention on climate change (UNCCC), the international maritimeorganization is regulating legal means of the reduction of greenhouse gas emissions from ships [1]. Research on technology development for improving energy efficiency of ships is required due to the energy efficiency design index (EEDI) was set as a mandatory requirement and has been applied to all ships built since 2013 [2].

The application of the hybrid electric propulsion system (HEPS) to the conventional ships is effective for improving energy efficiency [3]. The hybrid propulsion ship (HPS) consists of the HEPS with the hybrid power supply system (HPSS), rim driven propulsion drive system (RDPDS) and steering system (SS). RDPDS and SS include a motor and an inverter. HPSS consists of a diesel generator, an AC/DC converter (CNV), DC/DC CNV and a battery as shown Fig. 1. In the case of the mechanical propulsion ships, the main steam of propulsion machinery was diesel engines. On the other hand, hybrid propulsion ships are propelled by electric drive systems [4]. Various types of propulsor such as an electric podded azimuth thruster and rim driven propulsor have been developed for use in electric drive systems with electric motors [5]. These electrical systems must be verified prior to maritime demonstration because it affects the ship maneuverability. The ship maneuvering performances using the mathematical modeling group (MMG) model are different from the actual operating responses of the ship because it considers only hydrodynamic force and not the dynamic characteristics of the HEPS [6]. The evaluation of ship maneuvering performances considering the electro-dynamic characteristics of the HEPS with a high control frequency has a disadvantage of a long simulation time [7]. The modeling and simulation [3] have a problem of low accuracy on evaluate dynamic characteristics of HPS because it did not take into account the hydrodynamic forces of ship turning. To solve this problem, this paper proposes a simplified model considering the hydrodynamic forces generated from the turning of the ship to improve the computation speed. In addition, the hardware in the loop simulator (HILS) using ship dynamic model and the developed equipment is proposed to evaluate the electro-dynamic characteristics of HPS. The validity of the proposed model on HILS is verified by comparing with a detailed model on the electronic circuit simulation software (ECSS).

✉ Sung-An Kim
sakim@komeri.re.kr

[1] Korea Marine Eqiupment Research Instititue, Ulsan, Ulsan, Republic of Korea

Fig. 1 Configuration of HPS

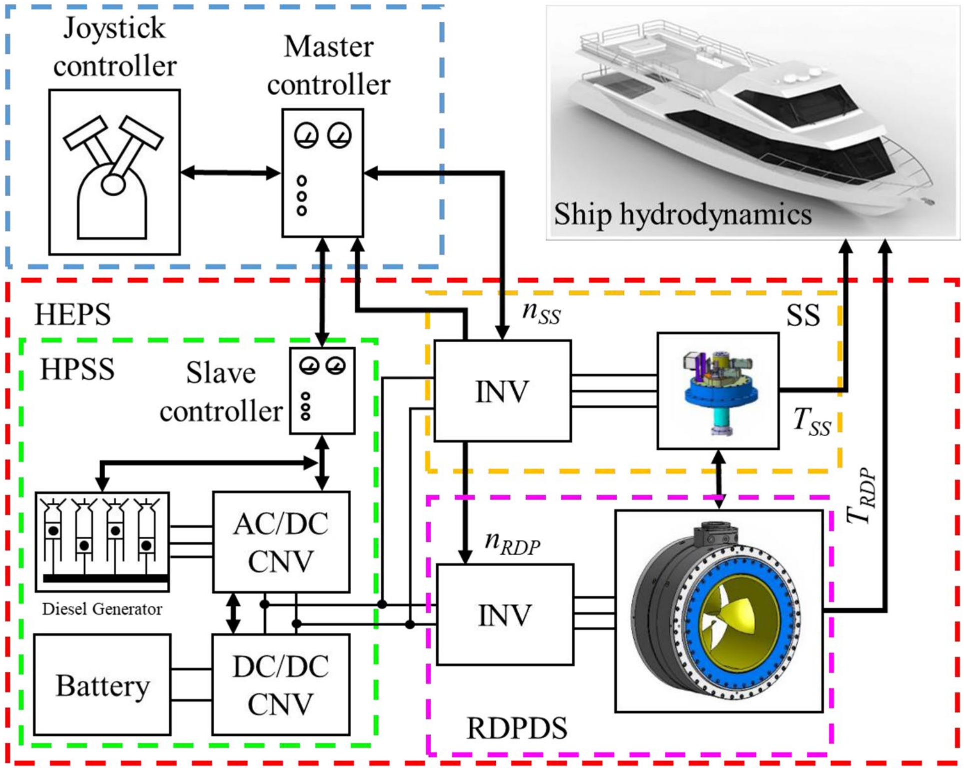

2 Simplified model of HPS

Figure 2a shows the preliminary experimental setup of HEPS. The master controller (MC) controls and monitors the RDPDS, SS, and HPSS. This setup only allows verification of simple operation between systems because of the no load conditions without fluid load. Therefore, HILS with ship HEPS model and ship dynamic model is needed for verifying HPS maneuverability. HPS model is classified as HEPS model and MMG model.

2.1 HEPS model

Figure 2b shows a block diagram of HEPS. This system is classified as the diesel generator, AC/DC CNV, DC/DC CNV, INV, RDPDS and SS. In RDPDS and SS, the generator and motor are both the surfaced permanent magnet synchronous machines (SPMSM). Therefore, they can be represented by the same simplified model using Park's transformation [8]. To simplify the model of PMSM, the voltage equations can be expressed as

$$\begin{aligned} v_d &= R_s i_d + \frac{\mathrm{d}\lambda_d}{\mathrm{d}t} - \omega_r \lambda_q \\ v_q &= R_s i_q + \frac{\mathrm{d}\lambda_q}{\mathrm{d}t} + \omega_r \lambda_d \end{aligned} \tag{1}$$

where R_s is phase resistance; i_d and i_q are d axis current and q axis current; λ_d and λ_q are d axis flux linkage and q axis flux linkage; and ω_r is angular velocity of rotor. The simplified model equations of AC/DC CNV using the rotor and rectifier reference frame [9] can be expressed by

$$\begin{aligned} \left\| \overline{v}^{\mathrm{rec}}_{\mathrm{d}q} \right\| &= \alpha(\cdot)\overline{v}_{\mathrm{g}} \\ \overline{i}_{\mathrm{dc}} &= \beta(\cdot)\left\| \overline{i}^{\mathrm{rec}}_{\mathrm{d}q} \right\| \end{aligned} \tag{2}$$

where $\alpha(\cdot)$ and $\beta(\cdot)$ are algebraic functions that can be obtained from the detailed simulation of the loading conditions. DC/DC CNV has boost mode for supplying power and buck mode for charging the battery. The simplified model equations of DC/DC CNV using the small signal model according to two modes [10] can be expressed by

$$\begin{aligned} L\frac{\mathrm{d}\hat{i}_{\mathrm{b}}}{\mathrm{d}t} &= \hat{v}_{\mathrm{b}} - D'\hat{v}_{\mathrm{g}} + V_{\mathrm{g}}\hat{d} \\ C\frac{\mathrm{d}\hat{v}_g}{\mathrm{d}t} &= D'\hat{i}_{\mathrm{b}} - \frac{1}{R}\hat{v}_{\mathrm{g}} + I_{\mathrm{b}}\hat{d} \end{aligned} \tag{3}$$

$$\begin{aligned} L\frac{\mathrm{d}\hat{i}_{\mathrm{b}}}{\mathrm{d}t} &= -\hat{v}_{\mathrm{g}} - D\hat{v}_{\mathrm{b}} + V_{\mathrm{g}}\hat{d} \\ C\frac{\mathrm{d}\hat{v}_{\mathrm{g}}}{\mathrm{d}t} &= \hat{i}_{\mathrm{b}} - \frac{1}{R}\hat{v}_{\mathrm{g}} \end{aligned} \tag{4}$$

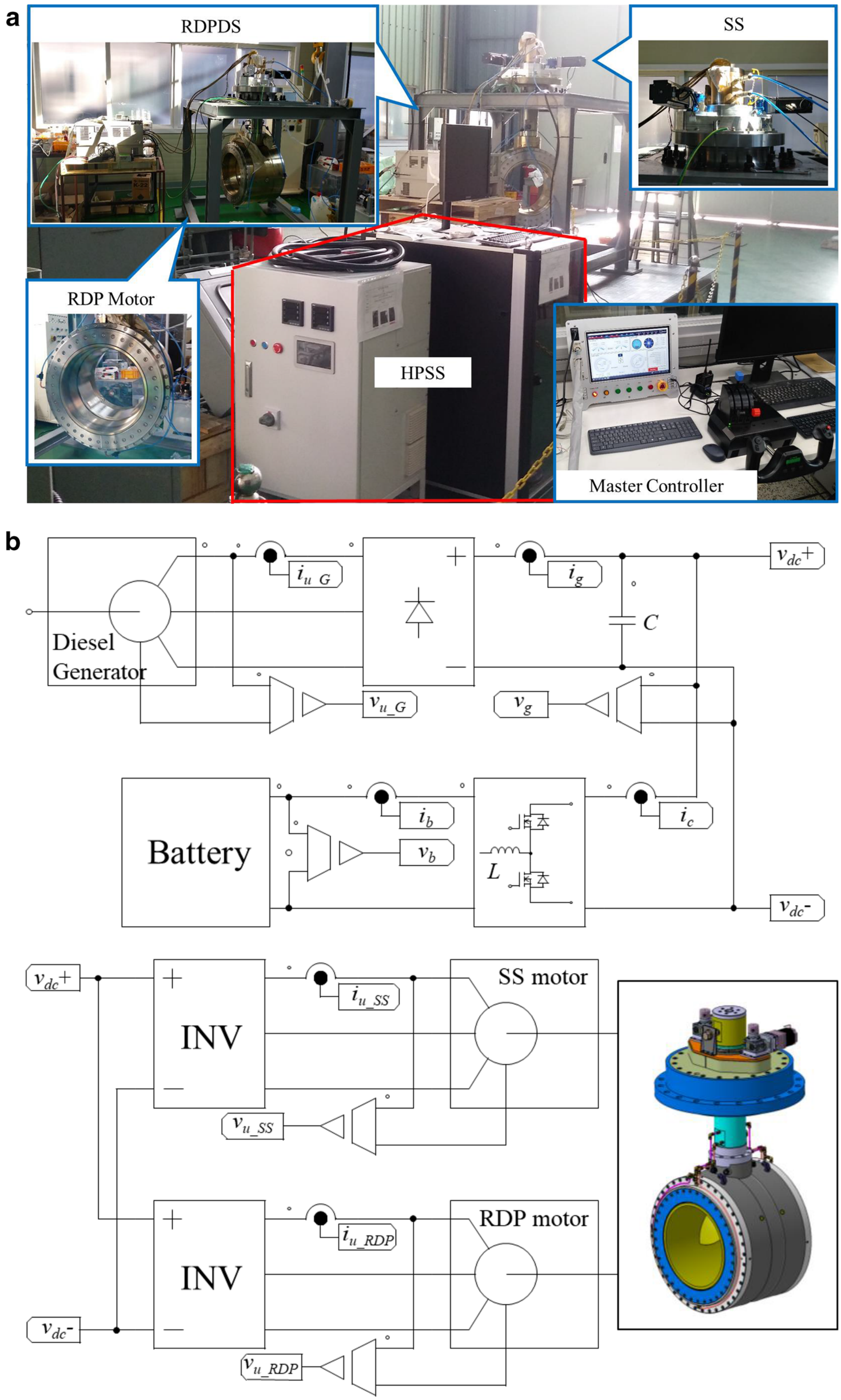

Fig. 2 HEPS. **a** Preliminary experimental setup, **b** block diagram

where the capital letter notations are the design operating point values. The simplified model equations of INV using an equipment stationary circuit by d–q transformation [11] can be expressed by

$$\begin{bmatrix} v_d \\ v_q \end{bmatrix} = \begin{bmatrix} \cos\left(\gamma_2 - \gamma\right) \\ \sin\left(\gamma_2 - \gamma\right) \end{bmatrix} \cdot m_i \cdot v_g$$
$$i_g = m_i \cdot \left(i_d \cdot \cos\left(\gamma_2 - \gamma\right) + i_q \cdot \sin\left(\gamma_2 - \gamma\right)\right) \tag{5}$$

where γ_2 and γ are the arbitrary initial phase angle and transformation angle; m_i is the modulation index; and v_g and i_g are the DC link voltage and current. The simplified model of the battery using the second order resistor capacitor battery equivalent circuit model [12] can be expressed by

$$\begin{aligned} v_b &= v_{oc(SOC)} - v_{p1} - v_{p2} - R_o \\ \dot{v}_{p1} &= -\frac{1}{R_{p1}C_{p1}}v_{p1} + \frac{1}{C_{p1}}i_b \\ \dot{v}_{p2} &= -\frac{1}{R_{p2}C_{p2}}v_{p2} + \frac{1}{C_{p2}}i_b \\ s\dot{o}c &= -\frac{1}{Q_n}i_b \end{aligned} \tag{6}$$

where v_b and i_b are the terminal voltage and current of battery; R_o is the ohmic resistance; R_{p1} and C_{p1} are the activation polarization resistance and capacitance; R_{p2} and C_{p2} are the concentration polarization resistance and capacitance. v_{p1} and v_{p2}, respectively, are the terminal voltage of C_{p1} and C_{p2}; and Uoc(soc) represents the open circuit voltage which is related with the value of state of charge.

2.2 MMG model

The motion equations of HPS can be expressed by the fixed earth coordinate system to define the position of the ship and the three axis forces such as surge X, sway Y and yaw Z [13]. A longitudinal distance x, transverse distance y and heading ψ using the three degree of freedom equations excluding the rolling motion of the ship can be expressed by

$$\begin{aligned} x &= \int u(t)\mathrm{d}t = \iint \left[\frac{X}{m} + vr + x_g r^2\right] \mathrm{d}t \\ y &= \int v(t)\mathrm{d}t = \iint \left[\frac{Y}{m} - ur - x_g \dot{r}\right] \mathrm{d}t \\ \psi &= \int r(t)\mathrm{d}t = \iint \left[\frac{Z}{I_z} - \frac{mx_g}{I_z(v + ur)}\right] \mathrm{d}t \end{aligned} \tag{7}$$

where u and v are the longitudinal and transverse velocities; and m and I_z are the ship mass and mass moment of inertia; x_g is the center gravity of ship; r is the rotational angular velocity around x_g; and $\dot{r}$ is the differentiation value of r. The components of the MMG model, the hydrodynamic forces and the ship moments can be expressed by

$$\begin{aligned} X &= X_H + X_P + X_R \\ Y &= Y_H + Y_P + Y_R \\ Z &= N_H + N_P + N_R \end{aligned} \tag{8}$$

where the subscripts H, P and R represent hull, propeller and rudder. The hydrodynamic force of hull can be expressed by a hydrodynamic derivative model that demonstrates the characteristics of the hull shape. The hydrodynamic force of the propeller cab be expressed by the thrust coefficient and torque coefficient based on the design specifications. The hydrodynamic force of rudder can be expressed by resistance reduction coefficient, force increase coefficient, additional lateral force [14].

The detailed equations for the elements of Eq. 8 are described in [15]. Finally, the simplified model of HPS can be composed of Eqs. 1–8 as shown Fig. 3.

3 Hardware in the loop simulator

To analysis the ship maneuvering performances of HPS, the MC based on the laboratory virtual instrument engineering workbench (LVIEW) was manufactured as shown Fig. 1. HILS is operated by applying the proposed model with HEPS model and MMG model to LVIEW. Figure 4a presents the flow chart of HILS. The parameters of ship and HPS are entered into the MC and then HILS is initialized

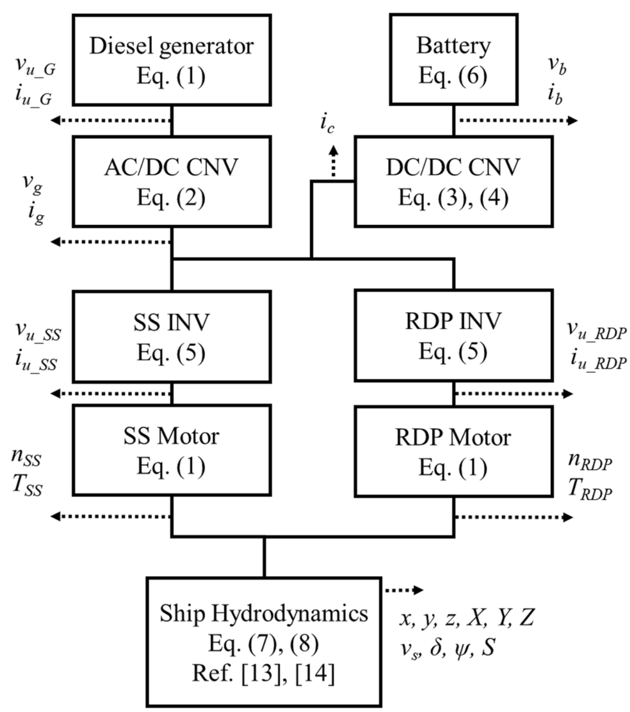

Fig. 3 Simplified model of HPS

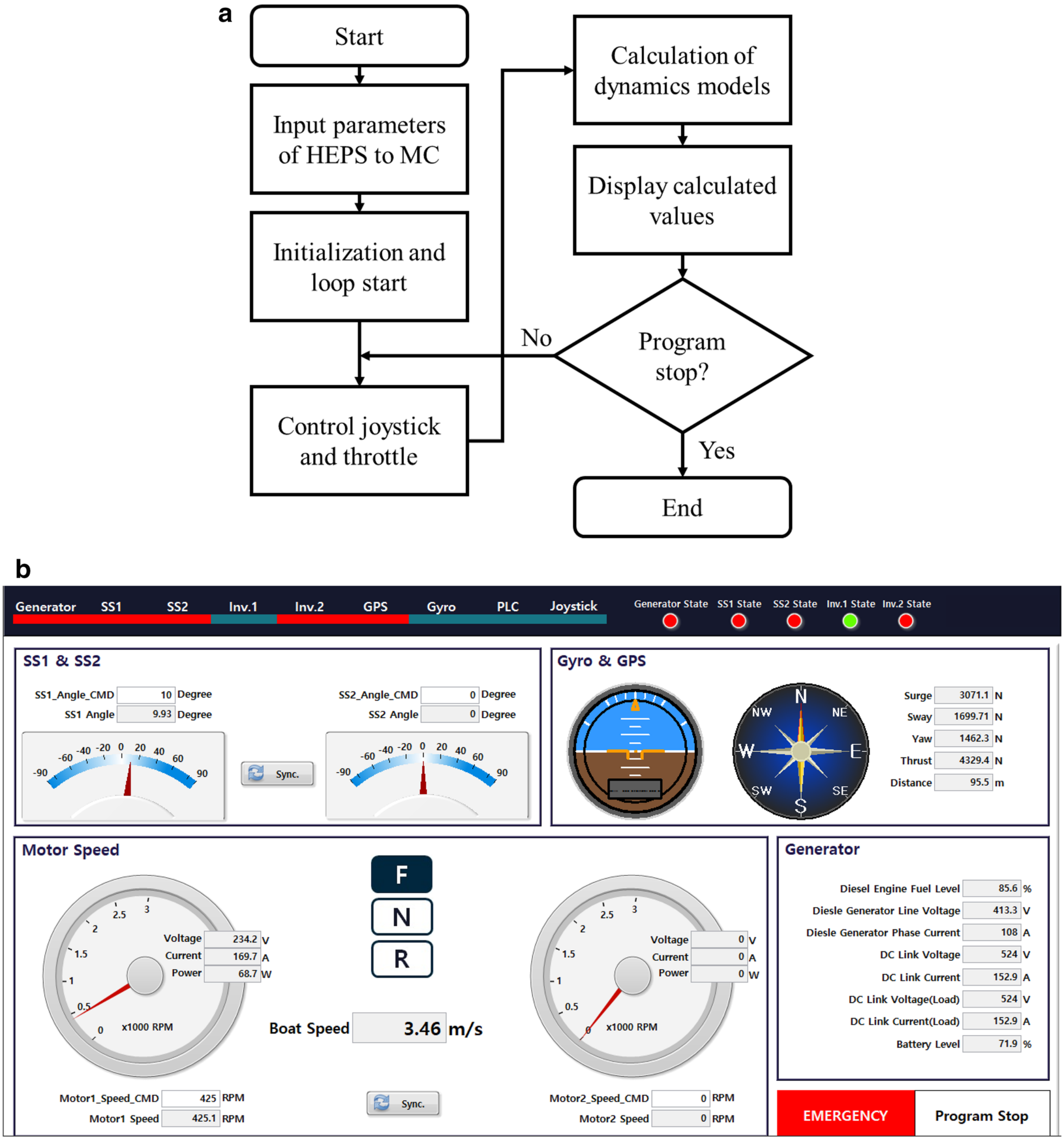

Fig. 4 HILS. **a** Flow chart, **b** control screen

and start an infinite loop at 1 s intervals. When the joystick or throttle is controlled, the dynamic model of HPS is calculated and displayed on control screen as shown Fig. 4b.

The difference between ECSS with the detailed model and LVIEW with the proposed model is the time step and sampling time to reduce the calculation speed. The time

Table 1 Specifications of ship

Item	Value
Length (L_{ship})	10 m
Ship speed (v_s)	4.3 m/s
Resistance coefficient (C_r)	0.012
Water density (ρ)	1025.9 kg/m^3
Lateral (A)	40 m^2
Weight (m)	5000 kg
Add mass (m_x, m_y, I_z)	747.5 kg, 762 kg, 80.5 kgm^2
Thrust reduction coefficient (t)	0.13
Wake (w)	0.13
K_t/K_q	2.53/1.18
Thrust (T)	6755 N
Torque of RDP (T_{r_max})	1386 Nm
Torque of SS (T_{s_max})	1931 Nm

Table 2 Parameters of HPS

Item	Value
Diesel generator	
Rated power	85 kW
Rated speed	1800 rpm
Rated voltage	380 V
AC/DC CNV	
Rated power	85 kW
Output voltage	DC 537 ± 10% V
DC/DC CNV	
Rated power	75 kW
High voltage	DC 537 ± 10% V
Low voltage	259 ~ 294 V
Battery	
Capacity	85 Ah
RDPDS and SS	
Rated speed	500/1150 rpm
Rated torque	1432.4/71.55 Nm
Rated power	75/10 kW
Phase resistance	4.99/0.517 mΩ
D/Q axis inductance	0.2/5 mH
Back EMF constant	557/389 V/krpm

step and sampling time of ECSS, respectively, are 10 µs and 1. If it is set smaller than these values, the accuracy of the dynamic characteristic is lowered due to the high control frequency required by detailed model. On the other hand, the time step and sampling time of LVIEW using proposed model can be set, respectively, 10 ms and 1 s to reduce the computation time.

4 Simulation

To verify the validity of the proposed model, HILS was performed to compare with the simulation results of the detailed model. The initial turning test, steady turning test and zigzag test were analyzed considering the operating conditions of HPS. Tables 1 and 2 show specifications and parameters of HPS. HPS is the 5-ton small sized ship with a maximum speed 4.3 m/s. The parameters K_t and K_q are thrust coefficient and torque coefficient [16, 17]. The hydrodynamic coefficient of the HPS used the ESSO tanker estimated coefficient [18]. Thrust at propeller speed 500 rpm is 6755 N and the calculated maximum RDPDS and SS torques are 1384 Nm and 1931 Nm, respectively. Therefore, the output power of RDP motor and SS motor including gear ratio 20 were selected as 75 kW and 10 kW considering the efficiency of each component. In the case of the diesel generator, 100 kW was selected considering the local load conditions and high speed mode. The battery capacity was selected to 75 Ah considering the sailing conditions of the ship.

4.1 Initial turning test

The initial turning test is to measure the moving distance of the ship when the heading reaches 10° by commanding 10° of rudder angle after reaching 85% of the maximum speed of the ship [19]. Figure 5 shows the comparison result of detailed model with ECSS and proposed model with LVIEW at initial turning test. v_s, δ and S are ship speed, rudder angle and moving distance; subscripts (D) and (P) are the detailed model and proposed model. Compared to the detailed model, the response of proposed model follows the general transient very well with the exception of some delay of δ.

4.2 Steady turning test

The steady turning test is to measure the advance distance and tactical diameter when the heading reaches 360° by commanding 35° of rudder angle after reaching 85% of the maximum speed of the ship [19]. N and T are speed of RDP motor and output torque of RDPDS and SS. Figure 6 shows the comparison result of detailed model and proposed model at steady turning test. The response of the proposed model

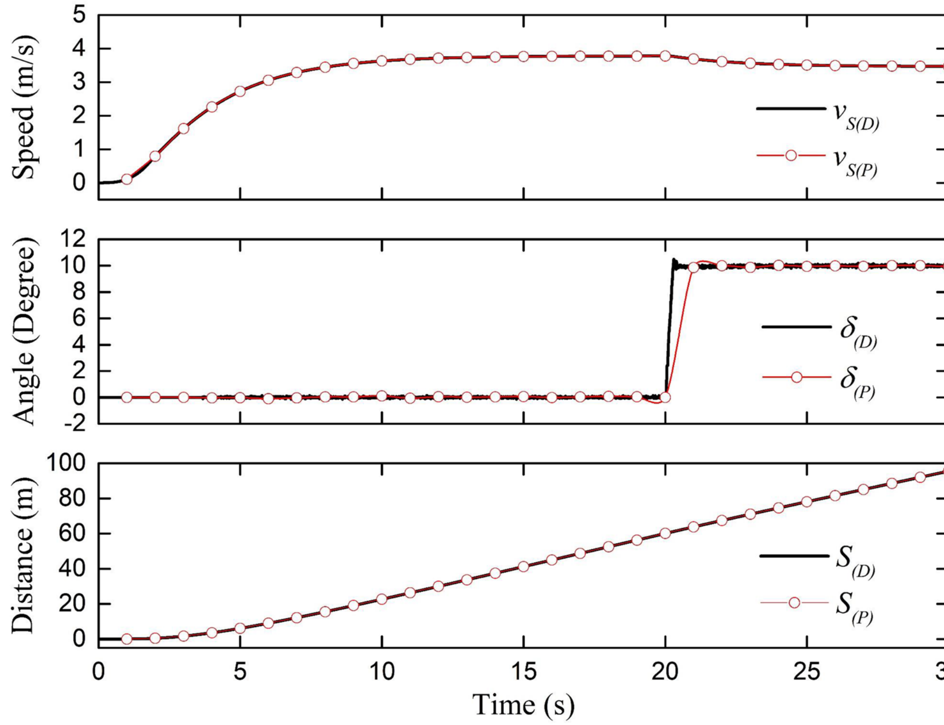

Fig. 5 Dynamic characteristics at initial turning test

follows almost exactly the trace produced by the detailed model during the entire transient with the exception of some initial overshoot of *X*, *Y*, *Z*.

4.3 Zigzag test

Zigzag test evaluates the overshoot angle, which is the transient heading by the zigzag steering method by 10° of the rudder angle [19]. Compared to the detailed model, the response of proposed model follows the general transient very well with the exception of some delay of v_s and δ as shown Fig. 7a. Figure 7b shows the output of RDP INV and SS INV. v_{u_RDP}, i_{u_RDP}, v_{u_SS} and i_{u_SS} are phase voltage and phase current of RDP INV and SS INV. v_{u_RDP} and i_{u_SS} have the high-frequency harmonics due to the INV switching. At the same time, the proposed mode contains only the high frequency noise due to the load variations, and it follows the overall transient envelope very well. Figure 7c shows the output values of HPSS. v_{u_G}, and i_{u_G} are phase voltage and phase current of the diesel generator; and i_C is output current of DC/DC CNV. Although Fig. 7c contains high frequency noise, the response of proposed model follows the general transient very well including the voltage fluctuations.

Table 3 shows the comparison results of computation time according to the models. The simplified model of HEPS greatly reduced the computation time of the proposed model. It can be used for the detailed operation verification of the developed hardware because the computation time period of the proposed model is in real time, as shown Fig. 4b.

5 Conclusion

To evaluate ship maneuverability, the combinations of HPS with slow response and HESS requiring fast control response require very long computation time without a simplified model. To solve this problem, this paper proposed a simpler approach to analysis ship maneuvering performances of HPS using HILS. In the proposed simplified model, the ship dynamic characteristics and HEPS are implemented in a proper state model from using the classical formulation, and presented simulator configuration based on LVIEW to reduce the long computation time of simulation with the high control frequency. As a result, the response characteristics and accuracy of the proposed model using LVIEW are excellent and the computation time of the simulation was greatly reduced compared with the detailed model using ECSS.

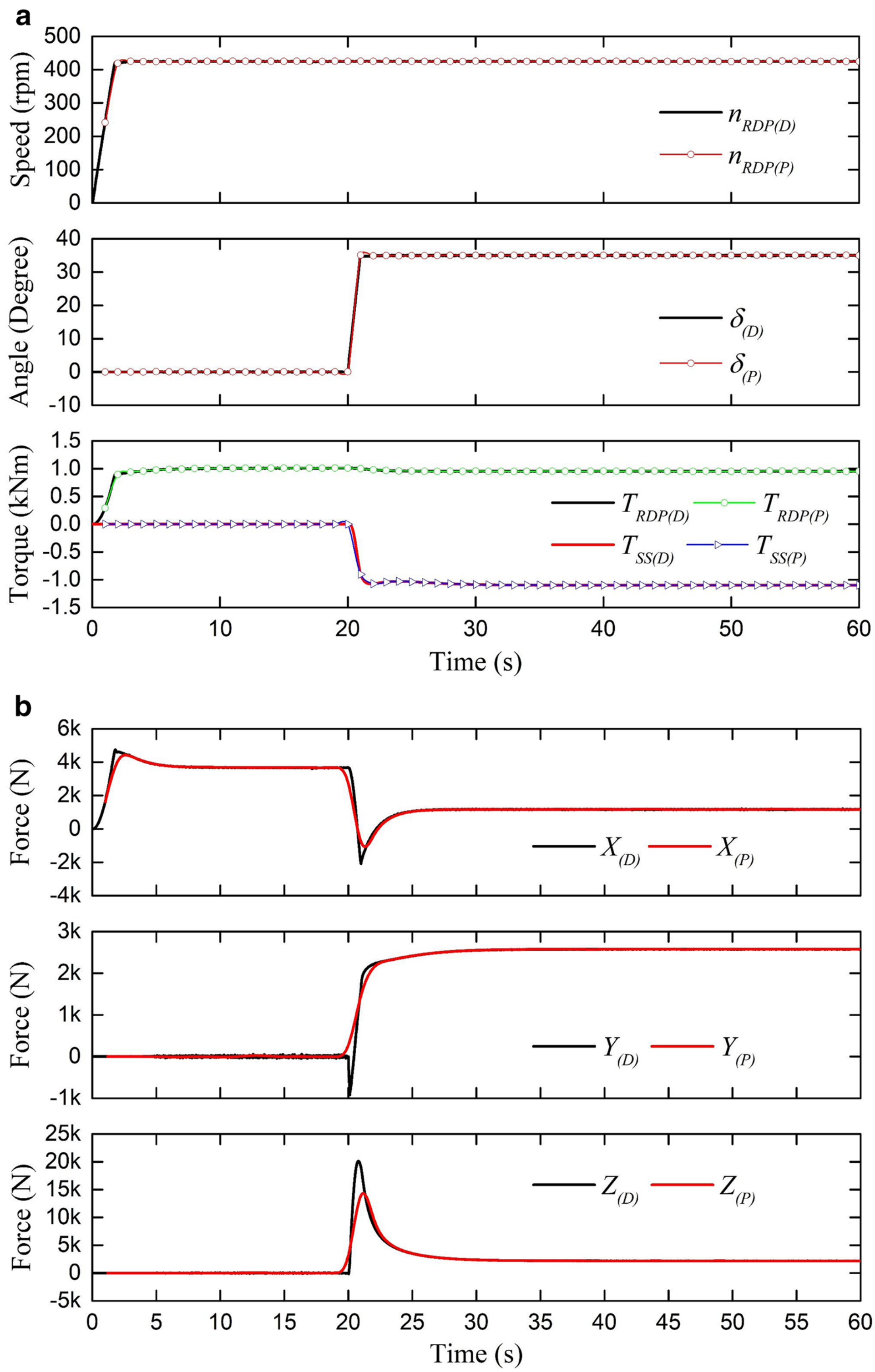

Fig. 6 Dynamic characteristics at steady turning test. **a** RDPDS and SS, **b** forces of ship

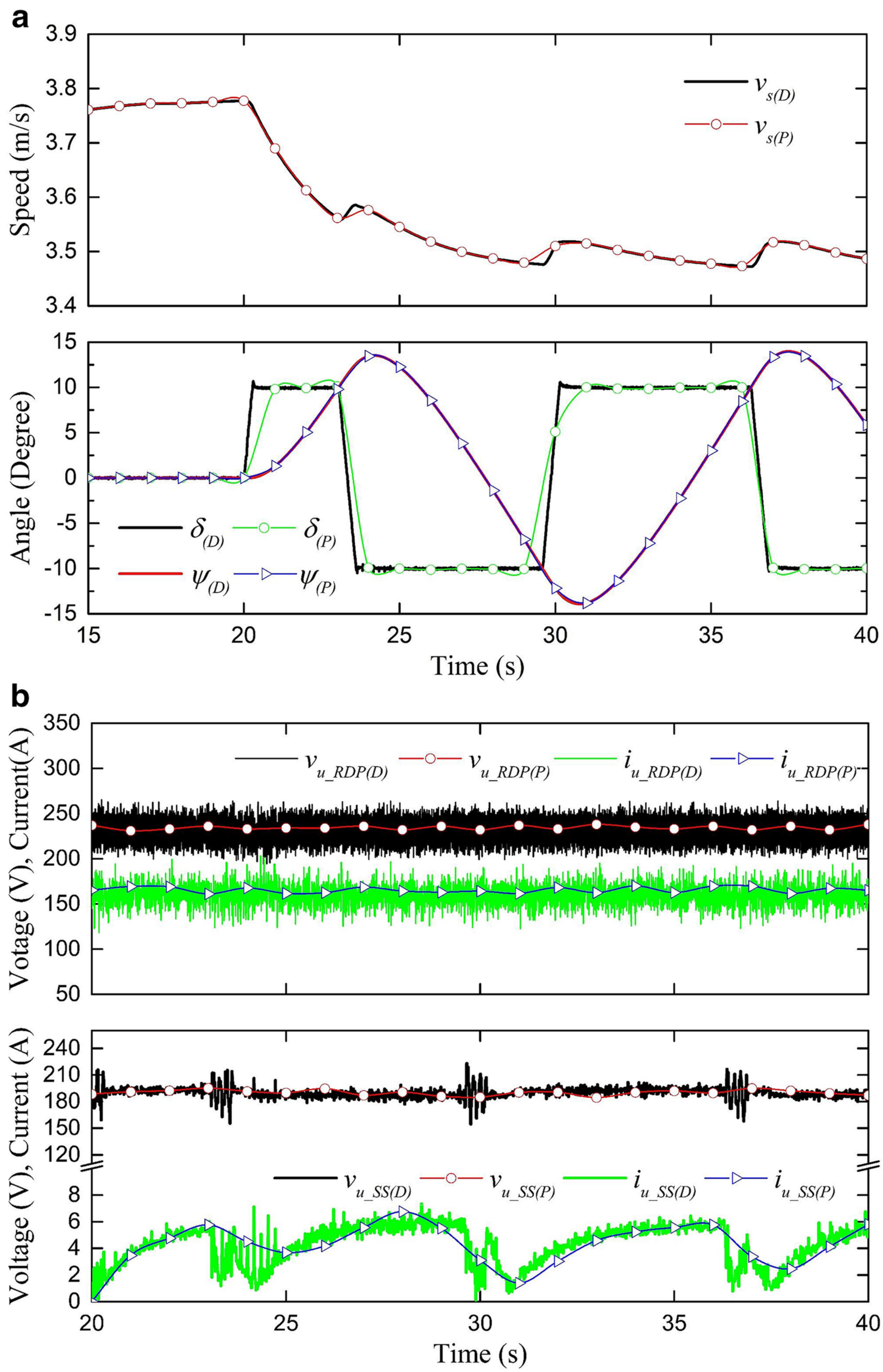

Fig. 7 Dynamic characteristics at zigzag test. **a** Ship, **b** RDP, **c** HPSS

Fig. 7 (continued)

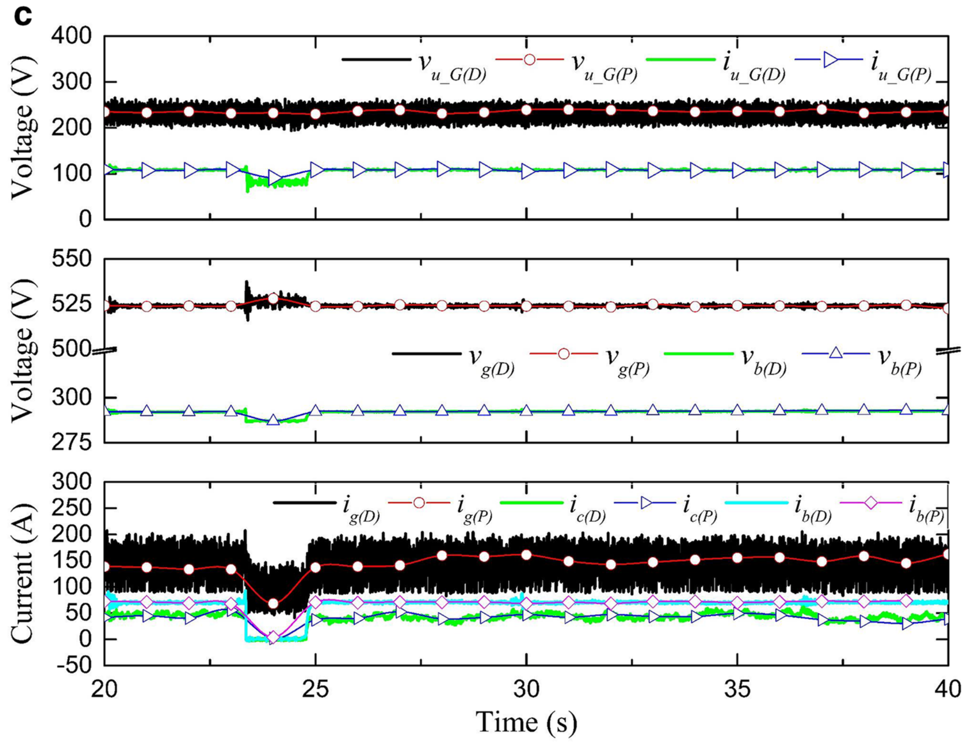

Table 3 Comparison results of computation time

Item	Detailed (min)	Proposed (s)
Initial turning test	27	30
Steady turning test	55	60
Zigzag turning test	39	40

References

1. Jung TH, Kang SG, Lee JG, Ahn JG (2018) International maritime organization (IMO) ship emission regulation trends and domestic and foreign measures. Bull Soc Naval Archit Korea 55(3):48–54
2. Kang GH, Kim SD (2017) Electric propulsion ship technology trend and power consumption analysis according to ship. Korean Inst Electr Eng 66(7):13–20
3. Zahedi B, Norum LE (2012) Modeling and simulation of all-electric ships with low-voltage dc hybrid power systems. IEEE Trans Power Electron 28(10):4525–4537
4. Hansen JF, Frank W (2015) History and state of the art in commercial electric ship propulsion, integrated power systems, and future trends. Proc IEEE 103(12):2229–2242
5. Lea M, Thompson D, Van Blarcom B, Eaton J, Friesch J, Richards J (2003) Scale model testing of a commercial rim-driven propulsor pod. J Ship Prod 19(2):121–130
6. Fang MC, Luo JH (2005) The nonlinear hydro ynamic model for simulating a ship steering in waves with autopilot system. Ocean Eng 32:1486–1502
7. Ku HK, Kwak KK, Kim JM (2015) A study integrated-power-system simulation model of all-electric-ship. Trans Korean Inst Power Electron 20(1):45–50
8. Kirtley JL, Beaty HW (1998) Electric motor handbook, chapter 6. McGraw-Hill, New York
9. Juri J, Pekarek Steven D, Ali D (2006) Parametric average-value model of synchronous machine-rectifier systems. IEEE Trans Energy Convers 21(1):9–18
10. Erickson RW, Maksimovic D (2007) Fundamentals of power electronics. Springer, Berlin
11. Rim CT, Choi NS, Cho GC, Cho GH (1994) A complete dc and ac analysis of three-phase controlled-current PWM rectifier using circuit d–q transformation. IEEE Trans Power Electron 9(4):390–396
12. Kim SA (2018) A study on the design and control of integrated power supply system with static transfer switch for special vehicle. Ph.D. Dissertation, Department of electrical engineering of Dong-A university.
13. Lee GW, Surendran S, Kim S (2009) Algorithms to control the moving ship during harbour entry. Appl Math Model 33(5):2474–2490
14. Kim SA, Hong KP, Lee SK, Kang GH (2020) Dynamic characteristics analysis of ship model considering RDP system. J Adv Mar Eng Technol 44(2):90–101
15. Lee HY, Shin SS (1998) Approximate technique for ship's maneuverability prediction. J Soc Naval Archit Korea 35(4):2474–2490
16. Molland AF, Stephen RT, Dominic AH (2017) Ship resistance and propulsion. Cambridge University Press, Cambridge
17. Kim DY, Kim YT (2019) Fundamental design of a 75-kw-rim-driven propeller. J Korean Soc Mar Eng 43(1):31–39
18. Kobayashi H, Blok JJ, Barr R, Kim YS, Nowicki J (2003) specialist committee on ESSO OSAKA: final report and recommendations to the 23rd ITTC. In: Proceedings of the 23rd International Towing Tank Conference, pp 8–14.
19. Lee CK (2005) A study on the evaluation and validation of IMO maneuverability standards of vessels. J Navig Port Res 29(5):365–370

Publisher's Note Springer Nature remains neutral with regard to jurisdictional claims in published maps and institutional affiliations.